

# InP/AlGaInP quantum dot semiconductor disk lasers for CW TEM<sub>00</sub> emission at 716 – 755 nm

Peter J. Schlosser,<sup>1,\*</sup> Jennifer E. Hastie,<sup>1</sup> Stephane Calvez,<sup>1</sup> Andrey B. Krysa,<sup>2</sup>  
and Martin D. Dawson<sup>1</sup>

<sup>1</sup>Institute of Photonics, University of Strathclyde, 106 Rottenrow, Glasgow G4 0NW, UK

<sup>2</sup>EPSRC National Centre for III-V Technologies, Department of Electronic and Electrical Engineering,  
University of Sheffield, Mappin Street, Sheffield S1 3JD, UK

\*[peter.schlosser@strath.ac.uk](mailto:peter.schlosser@strath.ac.uk)

**Abstract:** Multiple layers of InP QDs, self-assembled during epitaxial growth, were incorporated into the active region of an (Al<sub>x</sub>Ga<sub>1-x</sub>)<sub>0.51</sub>In<sub>0.49</sub>P based semiconductor disk laser with monolithic Al<sub>x</sub>Ga<sub>1-x</sub>As distributed Bragg reflector. Three gain structure samples were selected from the epitaxial wafer, bonded to single-crystal diamond heatspreaders and optically pumped at 532nm within a high finesse external laser cavity. Laser emission with peak wavelengths at 716, 729, and 739 nm, respectively, was achieved from the three samples; the latter demonstrating tuning from 729 to 755 nm. Maximum continuous wave output power of 52mW at 739nm was achieved with 0.2% output coupling; the threshold and slope efficiency were 220 mW and 5.7% respectively.

©2009 Optical Society of America

**OCIS codes:** (140.7270) Vertical emitting lasers; (140.5960) Semiconductor lasers.

---

## References and links

1. M. Kuznetsov, F. Hakimi, R. Sprague, and A. Mooradian, "Design and characteristics of high-power (> 0.5-W CW) diode-pumped vertical-external-cavity surface-emitting semiconductor lasers with circular TEM<sub>00</sub> beams," *IEEE J. Sel. Top. Quantum Electron.* **5**(3), 561–573 (1999).
2. S. Calvez, J. E. Hastie, M. Guina, O. Okhotnikov, and M. D. Dawson, "Semiconductor disk lasers for the generation of visible and ultraviolet radiation," *Laser Photon. Rev.* **3**(5), 407–434 (2009).
3. N. Schulz, J.-M. Hopkins, M. Rattunde, D. Burns, and J. Wagner, "High-brightness long-wavelength semiconductor disk lasers," *Laser Photon. Rev.* **2**(3), 160–181 (2008).
4. A. J. Kemp, G. J. Valentine, J. M. Hopkins, J. E. Hastie, S. A. Smith, S. Calvez, M. D. Dawson, and D. Burns, "Thermal management in vertical-external-cavity surface-emitting lasers: finite-element analysis of a heatspreader approach," *IEEE J. Quantum Electron.* **41**(2), 148–155 (2005).
5. B. Rudin, A. Rutz, M. Hoffmann, D. J. H. C. Maas, A.-R. Bellancourt, E. Gini, T. Südmeier, and U. Keller, "Highly efficient optically pumped vertical-emitting semiconductor laser with more than 20 W average output power in a fundamental transverse mode," *Opt. Lett.* **33**(22), 2719–2721 (2008).
6. J. Lutti, P. M. Smowton, G. M. Lewis, A. B. Krysa, J. S. Roberts, P. A. Houston, Y. C. Xin, and L. F. Lester, "740nm InP/GaInP quantum-dot laser with 190 A cm<sup>-2</sup> room temperature threshold current density," *Electron. Lett.* **298**, 41 (2005).
7. T. D. Germann, A. Strittmatter, J. Pohl, U. W. Pohl, D. Bimberg, J. Rautiainen, M. Guina, and O. Okhotnikov, "Quantum-dot semiconductor disk lasers," *J. Cryst. Growth* **310**(23), 5182–5186 (2008).
8. M. Butkus, K. G. Wilcox, J. Rautiainen, O. G. Okhotnikov, S. S. Mikhlin, I. L. Krestnikov, A. R. Kovsh, M. Hoffmann, T. Südmeier, U. Keller, and E. U. Rafailov, "High-power quantum-dot-based semiconductor disk laser," *Opt. Lett.* **34**(11), 1672–1674 (2009).
9. J. E. Hastie, S. Calvez, M. D. Dawson, T. Leinonen, A. Laakso, J. Lyytikäinen, and M. Pessa, "High power CW red VECSEL with linearly polarized TEM<sub>00</sub> output beam," *Opt. Express* **13**(1), 77–81 (2005).
10. A. B. Krysa, S. L. Liew, J. C. Lin, J. S. Roberts, J. Lutti, G. M. Lewis, and P. M. Smowton, "Low threshold InP/AlGaInP on GaAs QD laser emitting at ~740 nm," *J. Cryst. Growth* **298**, 663–666 (2007).
11. J. M. Hopkins, S. A. Smith, C. W. Jeon, D. Burns, S. Calvez, M. D. Dawson, T. Jouhti, and M. Pessa, "A 0.6W CW GaInNAs vertical external-cavity surface-emitting laser operating at 1.32μm," *Electron. Lett.* **40**(1), 30 (2004).

---

## 1. Introduction

Optically-pumped semiconductor disk lasers (SDLs), also known as vertical cavity surface emitting lasers (VECSELs) or optically-pumped semiconductor lasers (OPSLs), have shown a

dramatic increase in spectral coverage recently, due to the application of generic structural design and thermal management principles to a broad range of III-V semiconductor alloys. SDLs with Watt-level output power and characteristic high beam quality have been demonstrated at wavelengths from the red to the mid-infrared [1–5]. In addition, nonlinear frequency conversion techniques have provided selected coverage across the visible and into the ultraviolet [2]. Significant spectral gaps and regions of poor efficiency do remain, however, at the compositional and strain extremes between semiconductor alloy systems. Here, we address the important gap that exists between long-wavelength GaInP and short wavelength GaAs quantum well (QW) gain structure SDL's in the region 690 – 780 nm, for which we introduce gain structures based on InP quantum dots (QDs). Light in this spectral window is of interest for a range of applications including photodynamic therapy, sensing and biophotonics, for superior transmission through tissue and minimization of auto-fluorescence.

Quantum dots as laser gain media have generated a lot of interest, with desirable properties such as low threshold and low temperature sensitivity due to the discrete nature of the density of states. In addition, they allow the extension to longer wavelength emission over QWs since they enable the use of lower bandgap alloys with higher lattice mismatch. In recent work, Lutti et al. applied InP QDs within the gain region of electrically-injected edge emitting lasers to demonstrate room temperature emission at ~740 nm with record threshold current density of  $190 \text{ A cm}^{-2}$  [6]. Meanwhile, the feasibility of QD-based SDLs has been demonstrated with more widely-studied InAs QDs for emission wavelengths from 950 nm using submonolayer QDs to 1210 nm using QDs grown in the Stranski-Krastanow regime [7] and recently more than 4W output power has been demonstrated at 1032 nm [8]. Previously we have reported high power AlGaInP QW-based SDLs for emission up to 680nm [9]. The InP QD SDLs reported here are demonstrated to give circularly-symmetric  $\text{TEM}_{00}$  laser emission from 716 - 755nm and offer prospects for significant coverage in the red/deep red spectral region and into the near-ultraviolet by intracavity frequency doubling.

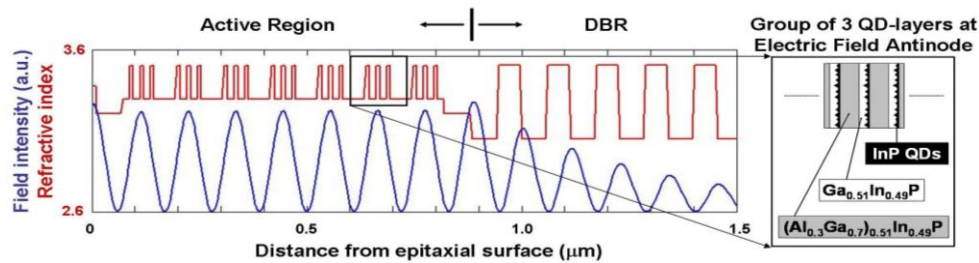


Fig. 1. Design of the SDL gain structure incorporating 7 x 3 layers of InP quantum dots within the resonant subcavity.

## 2. Design and growth

The SDL gain structure described in Fig. 1. consists of a multi-QD-layer active region directly on top of a distributed Bragg reflector (DBR), and was grown via metalorganic vapour phase epitaxy (MOVPE) in a low pressure (150 Torr) horizontal flow reactor with a non-rotating susceptor. The GaAs (100) substrate was misorientated  $10^\circ$  towards  $\langle 111 \rangle$  to achieve disordered growth [10]. Details of the layer compositions and thicknesses are given in Table 1. The growth temperature, common for all layers, was  $710^\circ \text{C}$ , with growth rates:  $\sim 7 \text{ \AA s}^{-1}$  for AlGaInP, GaInP and InP;  $\sim 7.2 \text{ \AA s}^{-1}$  for AlAs;  $\sim 10.2 \text{ \AA s}^{-1}$  for AlGaAs. The peak photoluminescence (PL) emission of the QDs measured from previous calibration growths was 740 nm, thus the DBR centre reflectivity and subcavity resonances were designed to match. The  $4\lambda$ -thick resonant subcavity, defined by the DBR and the semiconductor/air interface, absorbs  $\sim 98\%$  of the 532nm incident pump light (after reflection losses). A total number of 21 QD-layers were incorporated within the subcavity in groups of 3 layers at each of the 7 available electric field antinodes for resonant periodic gain (RPG). Each layer of self-assembled InP QDs, having a nominal thickness of  $\sim 6.2 \text{ \AA}$ , was deposited on top of the

$(\text{Al}_{0.3}\text{Ga}_{0.7})_{0.51}\text{In}_{0.49}\text{P}$  barrier material and capped by an 8-nm-thick  $\text{Ga}_{0.51}\text{In}_{0.49}\text{P}$  QW to form a dot-in-well (DWELL) structure. At either end of the active region a layer of composition  $(\text{Al}_{0.6}\text{Ga}_{0.4})_{0.51}\text{In}_{0.49}\text{P}$  provides additional carrier confinement and prevents carriers diffusing to the surface and recombining non-radiatively. A 10nm  $\text{Ga}_{0.51}\text{In}_{0.49}\text{P}$  cap prevents oxidation of the underlying layers.

**Table 1. SDL gain structure composition**

Layer	Composition	x	Thickness (nm)	Description
20	$\text{Ga}_x\text{In}_{1-x}\text{P}$	0.51	10	Cap
19	$(\text{Al}_x\text{Ga}_{1-x})_{0.51}\text{In}_{0.49}\text{P}$	0.6	58	Confinement
18	$(\text{Al}_x\text{Ga}_{1-x})_{0.51}\text{In}_{0.49}\text{P}$	0.3	16	Barrier
17 x 6	$6.2\text{\AA InP} + \text{Ga}_x\text{In}_{1-x}\text{P}$	0.51	8	QD + QW
16 x 6	$(\text{Al}_x\text{Ga}_{1-x})_{0.51}\text{In}_{0.49}\text{P}$	0.3	16	Barrier
15 x 6	$6.2\text{\AA InP} + \text{Ga}_x\text{In}_{1-x}\text{P}$	0.51	8	QD + QW
14 x 6	$(\text{Al}_x\text{Ga}_{1-x})_{0.51}\text{In}_{0.49}\text{P}$	0.3	16	Barrier
13 x 6	$6.2\text{\AA InP} + \text{Ga}_x\text{In}_{1-x}\text{P}$	0.51	8	QD + QW
12 x 6	$(\text{Al}_x\text{Ga}_{1-x})_{0.51}\text{In}_{0.49}\text{P}$	0.3	53	Barrier
11	$6.2\text{\AA InP} + \text{Ga}_x\text{In}_{1-x}\text{P}$	0.51	8	QD + QW
10	$(\text{Al}_x\text{Ga}_{1-x})_{0.51}\text{In}_{0.49}\text{P}$	0.3	16	Barrier
9	$6.2\text{\AA InP} + \text{Ga}_x\text{In}_{1-x}\text{P}$	0.51	8	QD + QW
8	$(\text{Al}_x\text{Ga}_{1-x})_{0.51}\text{In}_{0.49}\text{P}$	0.3	16	Barrier
7	$6.2\text{\AA InP} + \text{Ga}_x\text{In}_{1-x}\text{P}$	0.51	8	QD + QW
6	$(\text{Al}_x\text{Ga}_{1-x})_{0.51}\text{In}_{0.49}\text{P}$	0.3	16	Barrier
5	$(\text{Al}_x\text{Ga}_{1-x})_{0.51}\text{In}_{0.49}\text{P}$	0.6	64	Confinement
4	AlAs		60	DBR
3 x 40	$\text{Al}_x\text{Ga}_{x-1}\text{As}$	0.35	51.5	DBR
2 x 40	AlAs		60	DBR
1	GaAs		500	Buffer

### 3. Experimental details and results

#### 3.1 Wafer characterization

Prior to growth of the SDL gain structure, a calibration growth run of the gain region without the DBR was carried out and the room temperature photoluminescence is shown in Fig. 2. The substrate was not rotated during epitaxial growth of the SDL gain structure resulting in non-uniformity of the layer thicknesses across the wafer. Reflectivity measurements undertaken at room temperature revealed that the centre of the DBR stopband under these conditions varied from 718 – 770nm, with the subcavity resonance wavelength, indicated by a dip in the reflectivity, typically positioned at the centre of the stopband. Photoluminescence, excited by pumping at 532nm and collected at normal incidence to the sample surface, had a characteristic peak at the subcavity resonance wavelength. The non-uniformity of the wafer allowed the selection of gain structure samples with varying resonance offsets. Three samples, A, B, and C, were cleaved from the wafer with subcavity resonance wavelengths of 733, 745 and 750 nm, respectively (see Fig. 2). Also shown is the free-running emission spectrum of the SDL for each sample, which will be discussed in the following section.

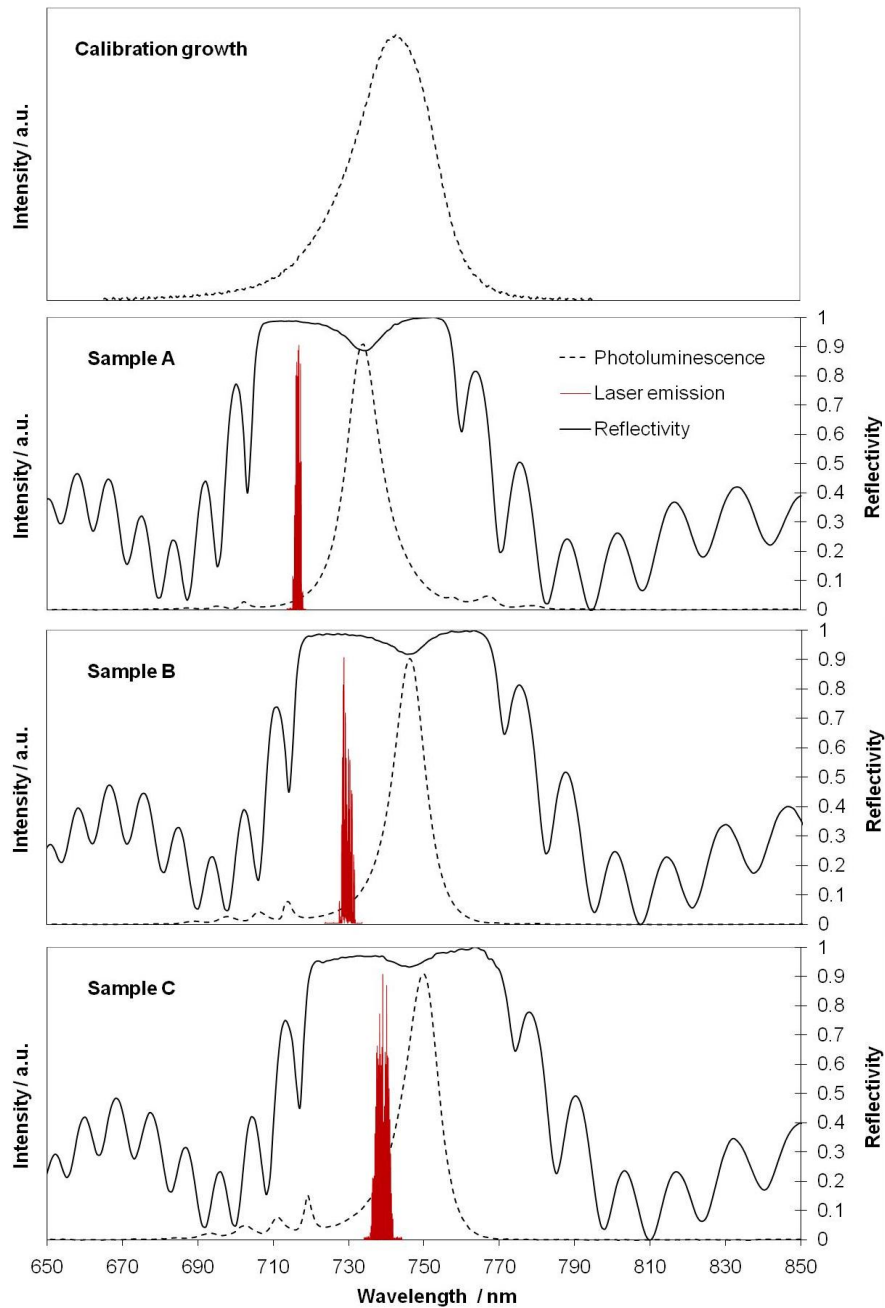


Fig. 2. Room temperature photoluminescence of the gain region calibration growth (top) and room temperature reflectance (bold) and photoluminescence (dashed) measurements for all three samples from the SDL gain structure. Also shown are the respective free-running SDL emission spectra.

### 3.2 Laser performance

In order to assess laser performance, a 'standard' 3-mirror resonator was set up, consisting of the SDL gain structure sample to be tested as one end mirror, a highly reflecting (HR) curved

folding mirror of 100 mm radius of curvature and a plane HR end mirror. A commercial frequency-doubled Nd:YVO<sub>4</sub> laser was used to optically-pump the SDL with up to 2.5W at 532 nm. The pump spot was ~74 μm in diameter with the SDL cavity aligned to match the intra-cavity mode; cavity arm lengths were, from the sample, 55mm and 270mm. For efficient thermal management, each sample was mechanically polished to remove ~150μm of the substrate (initial substrate thickness: 400μm) before a 500-μm-thick single crystal diamond heatspreader [11] was optically bonded to the intra-cavity surface. The sample and heatspreader were clamped in a brass mount kept at 7 °C via water cooling.

This arrangement yielded a near diffraction limited, circularly symmetric TEM<sub>00</sub> output beam profile with M<sup>2</sup> measured to be less than 1.1. The SDL incorporating, in turn, gain structure samples A, B and C had centre emission wavelength of 716, 728 and 740 nm, respectively. The free running laser emission spectra in each case, shown in Fig. 3a, are modulated by the etalon effect of the diamond heatspreader with a fringe peak separation of ~0.2 nm.

A 1-mm-thick birefringent filter (BRF) was placed at Brewster's angle in the long arm of the cavity. By rotation of the BRF, a tuning range of 26 nm from 729 to 755 nm could be achieved using sample C (see Fig. 3b). Also shown is an example of the narrowed laser output spectrum with the BRF rotation angle set for transmission near the peak of the available tuning range (~732 nm). The FWHM of the spectrum is less than 0.05 nm, limited by the resolution of the optical spectrum analyser.

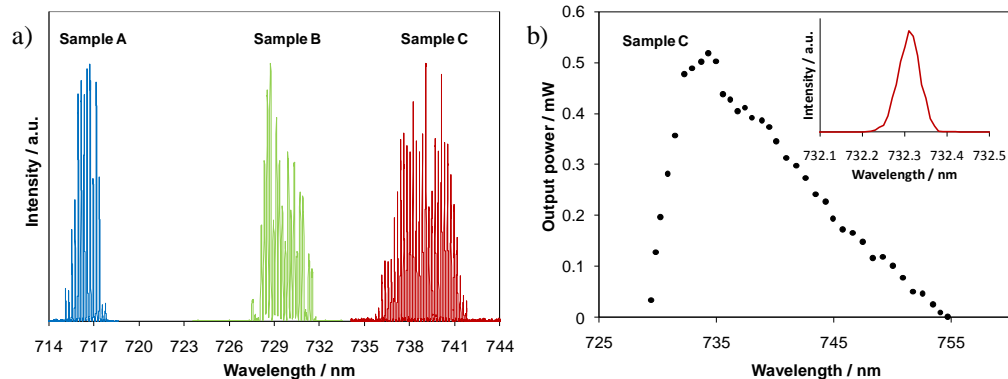


Fig. 3. SDL emission spectra. a) Emission spectra of the free-running SDL incorporating gain structure samples A, B, and C. b) Tuning curve obtained with sample C by insertion and rotation of an intracavity birefringent filter in an all-HR mirror cavity. Inset: an example of the narrowed laser emission spectrum during tuning.

The plane HR end mirror was replaced with an output coupler with measured transmission  $0.22 \pm 0.02\%$  across the wavelength range of interest. Power transfer measurements were taken for the SDL incorporating each sample in turn (see Fig. 4). Laser characteristics are summarized in Table 2. The slope efficiency for all samples is ~5%, however the threshold, and by implication the transparency carrier density, varies with the emission wavelength, most likely due to variation of the overlap with the QD peak gain. Thermal rollover occurs for ~1.5W pump power for all samples, so that the highest output power, 52 mW, is achieved for the sample (C) with the lowest pump threshold (220mW).

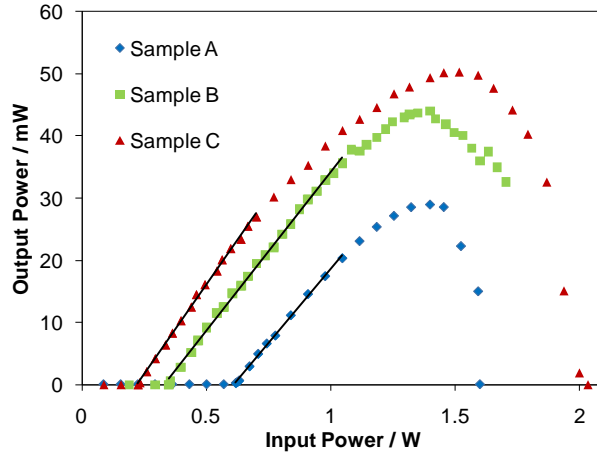


Fig. 4. Power transfer measurements for the SDL incorporating each gain structure sample. A linear fit to the data as shown was used to calculate the threshold and slope efficiency before rollover. Output coupling was 0.2%.

**Table 2. Summary of SDL characteristics using different gain structure samples**

Sample	Subcavity resonance $\lambda$ (nm) <sup>1</sup>	Laser emission $\lambda$ (nm) <sup>2</sup>	Threshold (mW) <sup>3</sup>	Slope Efficiency (%) <sup>3</sup>
A	733	716	610	4.8
B	745	729	330	5.1
C	750	739	220	5.7

<sup>1</sup>Measured via surface photoluminescence at room temperature.

<sup>2</sup>Free-running laser.

<sup>3</sup>Calculated via a linear fit to the data before rollover.

#### 4. Conclusions

InP quantum dot gain structures have been investigated, for the first time to our knowledge, as a means to extend the wavelength coverage of semiconductor disk lasers into the applications-rich spectral gap between 690 and 780nm. Multiple layers of InP quantum dots embedded within InGaP quantum wells were incorporated into an AlGaInP gain region grown on top of an AlGaAs distributed Bragg reflector. Laser emission from 716 – 755 nm with wavelength tuning up to 26nm was demonstrated using different samples from a spatially graded gain structure. The threshold power was shown to increase with increasing offset between the laser operating wavelength and the peak emission wavelength of the QD distribution. The mechanism responsible for setting the laser wavelength is as yet unidentified, however it is believed to be due to non-optimised overlap of the sub-cavity resonance and the QD gain. For this particular gain structure, the emission wavelength was, on average, ~14 nm shorter than the measured surface photoluminescence peak. This first demonstration opens the way to a range of novel red/deep red and (via intracavity second harmonic generation) near-ultraviolet tunable laser sources. Improved output power and slope efficiency may be expected via the optimization of the number of quantum dot layers and the overlap of the resonances with the QD distribution.

#### Acknowledgements

The authors would like to thank Peter M. Smowton of the University of Cardiff for helpful discussions. This work was supported by the Engineering and Physical Sciences Research Council, UK under grant no. EP/E056989.